Equation for Slip of Simple Liquids at Smooth Solid Surfaces

Hugh Spikes*

Mechanical Engineering Department, Imperial College of Science Technology and Medicine, London SW7 2AZ, U.K.

Steve Granick

Department of Materials Science and Engineering, University of Illinois, Urbana, Illinois 61801

Received January 23, 2003. In Final Form: March 30, 2003

We consider and develop mathematically a new equation for Newtonian fluid flow in the presence of slip at a solid surface. Slip is envisaged to occur only when a critical surface shear stress is reached, and once slip begins, it takes place at a constant slip length. Three instances are explored theoretically: slip possible at one surface only, slip possible at both surfaces with equal facility, and slip possible at both surfaces with differing facility. Quantitative comparison is made to experiments using the surface forces apparatus, and it is shown that this new slip model is able to reconcile results from different experimental studies.

Introduction

One of the ironies of the study of moving fluids is the long-standing doubt about the appropriate boundary condition. It is an empirically driven problem; one hardly questions that a jet of fluid flows through air with small frictional loss but that this is impossible for flow through a pipe. Textbooks and the mathematical descriptions of fluid flow assign the difference to different boundary conditions—the jet "slips" through air but "sticks" to the pipe, in the sense that fluid molecules immediately at the wall have no net velocity tangent to it.[1,2] These terms are not to be taken literally, as it would be unreasonable to expect the continuum description to carry microscopic information. We mean simply that the continuum description based on the "no-slip" boundary condition is held to describe the available data. Similarly, when we refer to "slip", we mean that data are inconsistent with "no-slip". The statement is not intended to carry microscopic information.

The "no-slip" assumption, i.e., that the immediate layer of liquid next to a solid surface moves with the same tangential velocity as the solid surface itself, is employed almost universally when analyzing fluid flow past solid surfaces and stands as the bedrock for much sophisticated calculation in fluid mechanics. Despite this, there have been persistent doubts for over a century about its validity.[1−5] These doubts have crystallized during the last 3 or 4 years with studies by a number of workers using several different experimental approaches which show convincingly that a variety of simple, Newtonian liquids can slip against solid surfaces.[6−16]

In many of these experiments the solid surfaces were very smooth;[6−11,13,14,16] this is understandable when one considers that very general arguments predict that the local instabilities of fluid flow near a rough surface should promote conditions that, in a continuum description, are describable by the no-slip boundary condition.[11] Contrarily, slip has also been observed when the surface is so rough that pockets of air are trapped between the surface and the fluid moving past it.[15] Furthermore, for some time it was believed that slip past very smooth surfaces was limited to cases where the surface was incompletely wetted by the fluid, but recent experiments demonstrate that this is not so. Slip can also occur in instances where very smooth surfaces are wetted completely by the moving fluid.[8,14]

It has been well-known for many years that some complex and/or highly non-Newtonian liquids such as polymer melts show effective slip at solid surfaces, due to an effective reduction in the viscosity of the fluid layer close to the surface resulting from shear thinning or compositional variation.[17−20] In these cases, slip has been successfully modeled by the Navier slip length model, which in Couette flow treats the liquid as flowing conventionally against a fictitious surface one "slip length", b, below the actual solid surface. This model relates the velocity at which the liquid slips, u_s, to the shear stress,

(1) For an historical review, see: Goldstein, S. *Mechanics of Fluids*; Clarendon Press: Oxford, 1938; Vol. II, pp 677−680.
(2) Vinogradova, O. I. *Int. J. Miner. Process.* **1999**, *56*, 31−60.
(3) Debye, P.; Cleland, R. L. *J. Appl. Phys.* **1958**, *30*, 843−49.
(4) Ruckenstein, E.;Rajora, P. *J. Colloid Interface Sci.* **1983**, *96*, 488−493.
(5) Churaev, N. V.; Sobolev, V. D.; Somov, A. N. *J. Colloid Interface Sci.* **1984**, *97*, 574−581.
(6) Pit, R.; Hervet, H.; Leger, L. *Tribol. Lett.* **1999**, *7*, 147.
(7) Boehnke, U.-C.; Remmler, T.; Motschmann, H.; Wurlitzer, S.; Hauwede, J.; Fischer, Th. M. *J. Colloid Interface Sci.* **1999**, *211*, 243.
(8) Pit, R.; Hervet, H.; Leger, L. *Phys. Rev. Lett.* **2000**, *85*, 980.
(9) Zhu, Y.; Granick, S. *Phys. Rev. Lett.* **2001**, *87*, 096105.
(10) Baudry, J.; Charlaix, E.; Tonck, A.; Mazuyer, D. *Langmuir* **2001**, *17*, 5322.
(11) Zhu, Y.; Granick, S. *Phys. Rev. Lett.* **2002**, *88*, 106102.
(12) Tretheway, D. C.; Meinhart, C. D. *Phys. Fluids* **2002**, *14*, L9.
(13) Craig, V. S. J.; Neto, C.; Williams, D. R. M. *Phys. Rev. Lett.* **2001**, *87*, 054504.
(14) Bonaccurso, E.; Kappl, M.; Butt, H. J. *Phys. Rev. Lett.* **2002**, *88*, 076103.
(15) Watanabe, K.; Yanuar; Udagawa, H. *J. Fluid. Mech.* **1999**, *381*, 225−238.
(16) Zhu, Y.; Granick, S. *Langmuir* **2002**, *18*, 10058.
(17) Schowalter, W. R. *J. Non-Newtonian Fluid Mech.* **1988**, *29*, 25−36.
(18) Léger, L.; Raphael, E.; Hervet, H. *Adv. Polym. Sci.* **1999**, *138*, 185−225.
(19) Denn, M. M. *Annu. Rev. Fluid Mech.* **2001**, *33*, 265−287.
(20) Wang, S. Q. *Adv. Polym. Sci.* **1999**, *138*, 227.

10.1021/la034123j CCC: $25.00
Published on Web 05/03/2003

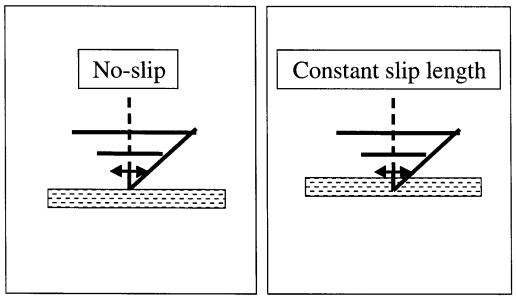

Figure 1. This figure distinguishes schematically between the no-slip boundary condition (left) and the Navier constant-slip boundary condition (right) in oscillatory flow. In both cases the velocity of the moving fluid (horizontal lines with arrows) extrapolates to zero. For no-slip, this occurs at the solid wall, but for slip, it occurs at a notional distance inside the wall and is finite where it crosses the wall.

τ_s, on the liquid at the interface and can be expressed as

$$\tau_s = \frac{\eta}{b} u_s \qquad (1)$$

where η is the dynamic viscosity of the liquid. Figure 1 compares no slip and slip at constant slip length schematically.

When slip was found to occur for simple Newtonian liquids, the results were naturally compared against this Navier model. However, for slip against very smooth surfaces, the outcome has been quite variable, with some workers obtaining results fitting closely to the constant slip length model[6,8,10] but others finding behavior quite at variance with this model.[9,13,14,16]

To help resolve this issue, a simple model for slip is presented here in which a critical shear stress criterion[21] is broadened to incorporate both a critical shear stress and a constant slip length criterion. This combined model is compared with experimental data from a crossed-cylinder mica−mica surface forces apparatus (SFA) and also used to reconcile the different forms of slip behavior seen in existing experimental studies.

Limiting Shear Stress Behavior

A surface forces apparatus was employed to study the hydrodynamic force generated between a pair of crossed mica cylinders lubricated by either tetradecane or water and subjected to oscillatory squeeze. In some experiments the mica surfaces were chemically modified, either by grafting on them a lyophobic monolayer of long chain octadecyltriethoxysiloxane (OTE)[9] or by adding a surfactant (1-hexadecylamine) to the tetradecane solvent.[16] Contact angle measurements showed that these treatments converted the normally fully wetted mica surfaces to ones only partially wetted by both test liquids.

For tetradecane between untreated, wetted mica, measured values of squeeze force were in accord with conventional Reynolds lubrication theory, which is based on the no slip boundary condition. However, when the mica was rendered lyophobic, the squeeze force, W, was drastically reduced, implying that the tetradecane flowed more easily from between the approaching mica surfaces than flow predicted by Reynolds theory. The occurrence of shear thinning or fluid structuring within the mica contact could be discounted, since the fluids were simple, low molecular weight liquids and reductions in squeeze force were measured even at quite large separations. The origin of this enhanced flow and consequent reduced squeeze force was therefore believed to be due to liquid slip.[9]

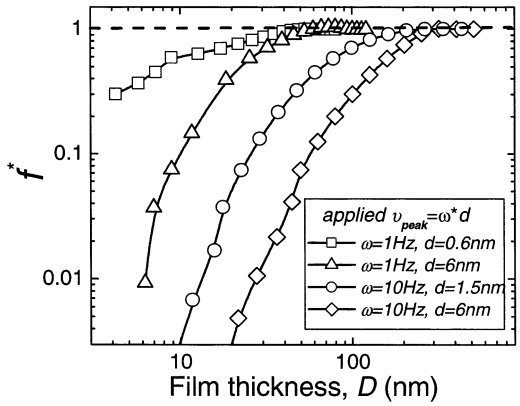

Figure 2. Figure adapted from ref 9 showing dependence of f^*, i.e., ratio of squeeze force measured in surface forces apparatus to that predicted from no-slip hydrodynamic theory, on minimum gap thickness D.[22] The system studied was water between two hydrophobic, crossed, 2 cm diameter mica cylinders at four applied peak squeeze velocities specified in the inset. At small values of D (denoted as h_o in the current paper), the squeeze force fell progressively below the no-slip prediction of unity, and this effect was greatest at high squeeze velocities.

This reduction in squeeze force can be expressed quantitatively by a parameter f^* introduced by Vinogradova,[2] which is the ratio of the measured squeeze force to that predicted assuming no-slip behavior. Figure 2 shows an example of the findings for water in which the parameter f^* is plotted against closest separation of the crossed cylinders. The data show that whereas $f^* = 1$ at the largest separations (in quantitative agreement with predictions based on the no-slip boundary condition), below a threshold separation the measured hydrodynamic forces became increasingly lower than those predicted from the no-slip boundary condition. Furthermore, the larger the peak velocity, the greater the separation at which deviation from no-slip behavior began. In these experiments, the peak velocity was defined as the product of the oscillatory squeeze radian frequency and the oscillatory amplitude.[22] A crossed-cylinder contact has the same film geometry as a ball-on-flat one, and for this geometry, Vinogradova has solved the equations of hydrodynamic flow for the case of liquid slip which obeys the constant slip length model of eq 1 at both surfaces.[23] She obtained the following analytical expression f^* (predicted ratio of slip to no-slip squeeze force)

$$f^* = \frac{h_o}{3b}\left[\left(1 + \frac{h_o}{6b}\right)\ln\left(1 + \frac{6b}{h_o}\right) - 1\right] \qquad (2)$$

In this equation b is the slip length and h_o is the minimum film thickness. The results of the experimental mica−mica study as illustrated in Figure 2 were very much at variance with Vinogradova's model. Equation 2 implies that f^* should be independent of the squeeze velocity, whereas, as shown in Figure 2, a strong dependence was observed. When eq 2 was applied to analyze the results, slip lengths were obtained that increased rapidly with increasing squeeze velocity and decreasing film thickness, to reach values in excess of 1 μm.[9]

(21) Spikes, H. A. *Proc. Inst. Mech. Eng., Part J* **2003**, *217*, 15.

(22) In ref 13, the velocity plotted in Figure 2 is the "applied velocity" (the velocity in the absence of a sample to resist it) and the true velocity was attenuated by apparatus compliance and hydrodynamic drag. As also noted elsewhere,[20] this distinction was not made clear in the text of ref 13. In the present paper, theoretical predictions are made to the true, attenuated velocity.

(23) Vinogradova, O. I. *Langmuir* **1995**, *11*, 2213.

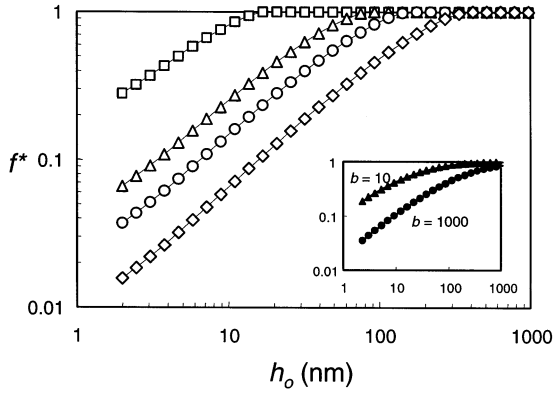

Figure 3. Dependence of hydrodynamic force ratio, f^*, on minimum gap thickness predicted from the critical shear stress for slip model with $\tau_{co} = 0.3$ Pa at four different peak squeeze velocities. Symbols are same as in Figure 2. Calculations were performed using the actual attenuated velocities, which were less than the applied velocity for reasons explained in footnote 22. The inset shows the prediction of the Vinogradova constant slip length b for slip model (eq 2) at two slip lengths b, 10 and 100 nm. The key point difference is that this model predicts f^* to be independent of squeeze velocity.

A recent interpretation by one of the authors[21] has suggested that these experimental results may represent not slip at constant slip length, but rather the onset of slip at a fixed, critical shear stress, τ_{co}. As shown in the Appendix, the shear stress on the fluid at the solid surfaces at radius r in no-slip, crossed-cylinder, or sphere-on-flat contact is given by

$$\tau_s = -3\eta w r/h^2 \tag{3}$$

where w is the downward squeeze velocity and h the fluid film thickness at radius r. A critical shear stress model for slip implies that, so long as the above shear stress does not reach the value τ_{co} anywhere within the contact, slip does not occur, but that wherever τ_{co} is reached, slip ensues at that location to maintain the surface shear stress at τ_{co}. In the sphere-on-flat squeeze contact without slip, the surface shear stress is zero at the center, rises to a maximum at $h = 4h_o/3$, and then decays quite rapidly with distance from the contact center. This means that, with a critical shear stress model, slip will be confined to an annular region around the center of the contact, quite unlike the constant slip length model where it will occur over the whole film.

For the case of slip at both surfaces, the critical shear stress for slip model yields an expression of pressure gradient of the fluid at radius r in the contact of the form[21]

$$\frac{dp_r}{dr} = -\min\left(\frac{6\eta w r}{h^3}, \frac{2\tau_{co}}{h}\right) \tag{4}$$

where the min function represents the minimum value of the two terms within the parentheses, the first term corresponding to the no-slip and the second to the slip condition. Because slip takes place over just some of the contact, this equation cannot be integrated analytically to derive a simple expression for the load support. However numerical integration to yield the pressure, the load, and f^* is very straightforward.

Figure 3 contrasts the form of f^* predicted by the critical shear stress model and the constant slip length model for the case of slip at two surfaces. The test conditions of viscosity, ball radius, and squeeze rates analyzed are the same as those used in a study by one of the authors,[9] and

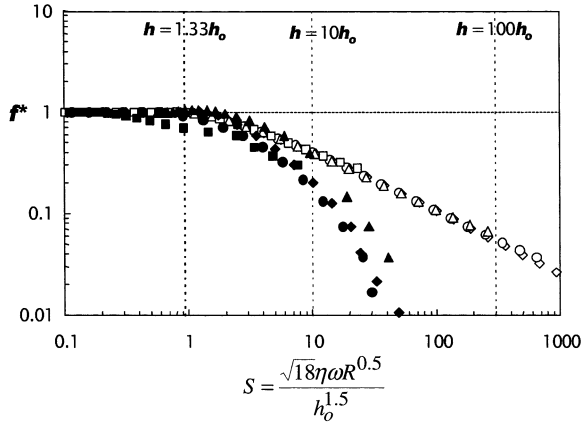

Figure 4. Dependence of hydrodynamic squeeze force ratio on the surface shear stress parameter S for both experimental data[9] (solid symbols) and the critical shear stress for slip model with $\tau_{co} = 0.3$ (hollow symbols) at all four squeeze velocities (same symbol shapes for squeeze velocity as in Figure 2). This representation collapses the data at different squeeze velocities. Slip begins at $h/h_o = 1.33$ when S exceeds 0.92 (dashed line). At S values greater than this, an annular region of slip forms, reaching from very close to the center of the contact out to some critical radius where the no-slip shear stress falls below 0.3. The other two vertical dashed lines show the predicted S values needed for the slipping zone to reach $h = 10h_o$ and $h = 100h_o$.

the predictions fit the form of those results quite well for a shear stress value $\tau_{co} \approx 0.3$ Pa. The model predicts both the measured dependence of f^* on squeeze velocity and also the quite sharp transition from nonslip to slip seen in the experimental results as h_o was reduced. The location of this transition is governed by the value of τ_{co}, since it occurs when the maximum surface shear stress reaches this value. Also shown in the inset of Figure 3 is the prediction of the constant slip length model of slip at two slip length values.

In any model of slip, an important operational parameter is likely to be the shear stress at the fluid/surface interface. In no-slip conditions this is given, at gap thickness h, by

$$\tau_s = \frac{18^{1/2}\eta w R^{0.5}}{h_o^{1.5}}\left(\left(\frac{h_o}{h}\right)^3 - \left(\frac{h_o}{h}\right)^4\right)^{1/2} \tag{5}$$

where R is the ball radius. The initial group of terms, $S = 18^{1/2}\eta\omega R^{0.5}/h_o^{1.5}$ in eq 5 thus summarizes how the overall contact parameters influence the surface stress. Figure 4 plots f^* against S for both the experimental data[9] and the limiting shear stress predictions from Figure 3. It can be seen that this plot collapses data at different squeeze velocities and provides agreement between measurement and prediction in the initial stages of slip.

New Slip Model

Unfortunately, while a critical shear stress for slip criterion describes these experimental results reasonably well, it is not in accord with studies that have been found to show slip at a constant slip length. The critical shear stress model outlined above implies that when slip takes place, it does so at effectively infinite slip length. Hence a new model is proposed that combines both features, a critical shear stress at which slip begins, followed by slip at a constant slip length. In this case, the shear stress when slip takes place is given by

$$\tau_c = \tau_{co} + \frac{\eta}{b} u_s \tag{6}$$

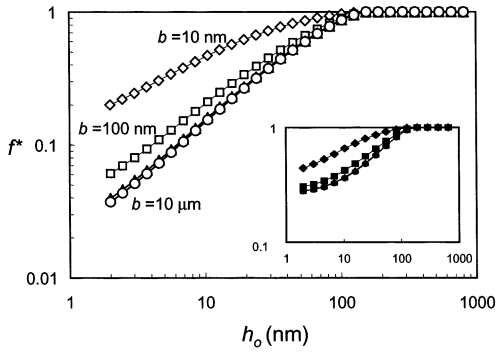

Figure 5. Dependence of hydrodynamic force ratio, f^*, on minimum gap thickness for combined limiting shear stress and constant slip length model (slip at both walls) for $w_{pk} = 100$ nm/s, $\tau_{co} = 0.3$ Pa, and four slip lengths as indicated (open triangles are $b = 1$ μm but are obscured by the $b = 10$ μm predictions). Notice that f^* is effectively independent of slip length at $b > 500$ nm. The inset shows predicted f^* for the case of slip at only one wall (same symbols as main figure). The predicted influence of slip on hydrodynamic squeeze force is much smaller in this case.

Possible physical origins of this model are considered briefly in the Discussion.

The Appendix shows how expressions for the pressure gradient in the ball-on-flat/crossed-cylinder contact can be derived for this slip model for the three cases of (i) slip possible at one surface, (ii) slip possible at both surfaces with equal facility, and (iii) slip possible at both surfaces with different facility. The pressure gradient equations obtained for the first two of these are as follows

(a) Slip possible at one surface only

$$\frac{dp_r}{dr} = -\min\left(\left(\frac{6\eta wr}{h^3}\right), \left(\frac{6\eta wr}{h^3} - \frac{6b}{(h+4b)}\left(-\frac{\tau_{co}}{h} + \frac{3\eta wr}{h^3}\right)\right)\right) \quad (7)$$

(b) Slip possible at both surfaces with equal facility

$$\frac{dp_r}{dr} = -\min\left(\left(\frac{6\eta wr}{h^3}\right), \left(\frac{6\eta wr}{h^3} - \frac{12b}{(h+6b)}\left(-\frac{\tau_{co}}{h} + \frac{3\eta wr}{h^3}\right)\right)\right) \quad (8)$$

At a given radius r within the fluid film, the pressure gradient can have either the first value in the outer bracket (corresponding to the no-slip case) or the second value (when slip occurs), whichever bracketed term is the smaller. The second bracketed term is only numerically smaller than the first when $3\eta wr/h^2 > \tau_{co}$. Equations 7 and 8 (and eq A31 for slip with different facility at either surfaces) can be very easily numerically integrated over the contact to obtain the pressure field and thus the load support and f^*.

Figure 5 shows predictions of this new model using several different slip lengths for one squeeze velocity condition. It can be seen that as the slip length is increased, the predictions approach one another and also the critical shear stress model. The inset shows comparable predictions for the case when slip can only occur at one of the surfaces.

To test the combined model, new SFA work has been carried out using the fluid ethylene glycol. The mica−mica crossed cylinders apparatus was the same as that employed in previous work,[9] and tests were carried out

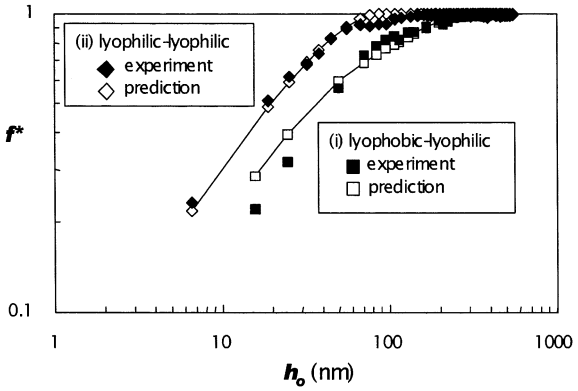

Figure 6. Comparison of experimental and predicted hydrodynamic force ratio, f^*, versus minimum film thickness for ethylene glycol (viscosity 17 cP) in two contacts, (i) lyophobic coated mica on lyophilic uncoated mica (squares) and lyophilic uncoated on lyophilic uncoated mica (diamonds). In the predictions, assumed slip criteria are $\tau_{co} = 1.3$ Pa, $b = 10$ μm at lyophobic surface, $\tau_{co} = 6$ Pa, $b = 100$ nm at lyophilic surface. The nominal peak squeeze velocity was 100 nm/s, but the actual value, which was monitored, was reduced at low h_o values by film damping for the reasons noted in footnote 22.

in two conditions, (i) between two mica surfaces where one was coated with a lyophobic monolayer of dodecanethiol on sputtered gold, using methods described elsewhere,[24] (ii) between two uncoated mica surfaces. In both cases slip was observed in thin film conditions, with slip occurring more easily in the coated/uncoated case than in the uncoated/uncoated one. Figure 6 shows the measured f^* versus minimum film thickness for the two cases. Also shown on this plot is the predicted f^* versus h_o behavior for the new slip model based on selected critical shear stress for slip and slip length values selected to give good fit between the experimental results and the model. The experimental results are consistent with slip occurring with a low τ_{co} value and a large slip length at the lyophobic surface, quite similar to the values found with tetradecane, and a higher τ_{co} and lower slip length at the lyophilic surface. It was not possible to obtain consistent fit to this pair of results using the critical shear stress for slip or the constant slip length model, but only with the combined model.

Discussion

The above work shows that the critical shear stress for the onset of slip, τ_{co}, is quite small, in the 0.1−2 Pa range for the lyophobic surfaces examined and ≈6 Pa for the lyophilic surface. This may be why it has not been observed in some studies, since its effect on flow behavior will only be apparent in low shear stress contacts, while in severe contact conditions, the second, constant slip length term will predominate. For example, a recent SFA study by Baudry et al., in which a lyophilic ball was oscillated against a lyophobic flat,[10] obtained squeeze results which were interpreted to obey the constant slip length model of Vinogradova,[23] with a slip length b of 38 nm. However it is found that the new, combined slip model with $b = 38$ nm and $\tau_{co} = 0.3$ Pa fits the data of Baudry and co-workers equally well. This is because they employed a high viscosity liquid (glycerol) and also a quite small radius of curvature contact. In combination, these two factors meant that a surface shear stress of 0.3 Pa was reached over most of the load-bearing region of the contact under all of the conditions tested, so that the second term in eq 6 overwhelmed the first.

(24) Zhang, X.; Zhu, Y.; Granick, S. *Science* **2002**, *295*, 663.

The influence of a τ_{co} term is also likely to be less evident in conditions where the shear stress is constant over the surface, as in capillary and Couette flow, than in geometries where it varies, as in the surface forces apparatus or atomic force microscope. In the former, a finite value of τ_{co} will merely offset the plot of strain rate versus slip velocity, and eq 6 will still yield a constant shear slip length.

One limitation of the proposed model is that it does not adequately fit the values of f^* measured for high surface shear stress conditions. For slip at both surfaces, Vinogradova's constant slip length, eq 2, and the combined criteria slip eq 6 both predict that under the most preferential slip conditions, the gradient of $\ln(f^*)$ vs $\ln(h_o)$ should reach a maximum value of unity. Contrary findings[9] imply either that slip velocity depends more strongly on surface shear stress than the normally assumed power of unity or that some factor in addition to surface shear stress controls slip. One possibility is that a critical shear stress controls the onset of slip (according to theory at $h = 4h_o/3$) and its initial development around this zone but that at some stage this slip region propagates across the contact to effectively remove the limiting shear stress condition at other regions.

Like the constant slip length model, the proposed model of slip is a purely mathematical one and it is of interest to consider how it might relate to physical behavior at the interface. There exist two main physical models of slip of simple liquids at smooth, lyophobic surfaces. One, due to Tolstoi, is based on the enhanced mobility of molecules of liquid immediately adjacent to a nonwetting solid.[25] The second, more recent suggestion, discussed by Vinogradova[23] and recently formalized by de Gennes,[26] is the formation of a nanothickness gas or vapor film of low shear strength between the liquid and the nonwetting solid surface. Both of these physical models have been shown to predict slip behavior that obeys the constant slip length equation.

So far as the authors are aware, no physical model based on a critical shear stress has been put forward with respect to the slip of simple liquids. In polymer flow however, where the recognition and study of slip is much more advanced, models incorporating both a critical shear stress and stress-dependent slip rate, resulting from a combination of chain debonding and disentanglement, have been developed.[18−20] In these, the onset of slip results from a sudden viscoelastic instability above a critical strain. Such a concept might be used to incorporate a critical shear stress for slip into a model of the Tolstoi type.[25] It is also not difficult to envisage the existence of a critical shear stress for slip in the gas film slip model. In this model, it has been conjectured that liquid strain close to the surface transforms small droplets of gas, which collect preferentially at the nonwetted surface, into an extended, thin film.[26] Such a transformation might well depend on the strain rate of the neighboring liquid and thus take place only when a critical shear stress condition is reached.

Conclusions

There is now strong experimental evidence that simple Newtonian liquids can slip against very smooth solid surfaces. However there is some debate about the most appropriate equation to describe this slip, with some work agreeing quite closely with the classical constant slip length equation but other results being greatly at variance with this model.

(25) Blake, T. D. *Colloids Surf.* **1990**, *47*, 135.
(26) de Gennes, P.-G. *Langmuir* **2002**, *18*, 3213.

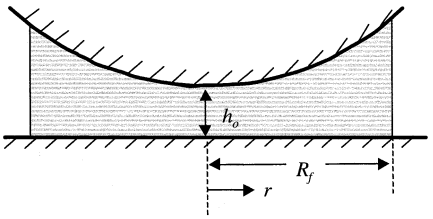

Figure 7. Geometry of ball-on-flat (or crossed-cylinder) contact showing notation used for calculations.

This paper has shown that some of the apparent differences in the form of slip behavior observed in different experiments can be reconciled if slip is envisaged to occur only when a critical surface shear stress is reached and that, once slip begins, it then takes place at a constant slip length. The suggested slip equation is as stated in eq 6 in this paper. In practice, because the critical shear stress is quite small, its effect will be negligible in experiments involving high shear stress conditions. However it will have a strong effect in low shear stress conditions and be particularly evident in conditions where the surface shear stress varies over the fluid film being studied, as is the case in the surface forces apparatus. It is also expected to have a strong effect in conditions where surface roughness "pins" the moving fluid up to a critical level of shear rate[11]

Acknowledgment. We thank Hyunjung Lee for performing the experiments with ethylene glycol. This work was partially supported by the U.S. Department of Energy, Division of Materials Science, under Award No. DEFG02-91ER45439 through the Frederick Seitz Materials Research Laboratory at the University of Illinois at Urbana-Champaign.

Appendix

The ball-on-flat or crossed-cylinder contact as shown in Figure 7 is centrosymmetric, with film thickness at radius r given to a close approximation by the parabolic form

$$h = h_o + \frac{r^2}{2R} \tag{A1}$$

where h_o is the central film thickness at $r = 0$ and R the radius of the sphere in contact with the flat. The contact is filled to a radius R_f with Newtonian fluid of dynamic viscosity η. The contact is subjected to a squeeze velocity of $w = -dh/dt$ due to downward motion of the upper surface.

The task is to determine the instantaneous normal force generated in the fluid film as a function of h_o, R, R_f, η, and w for a liquid film exhibiting slip at one or both surfaces described in terms of a slip model

$$\tau_c = \tau_{co} + \frac{\eta}{b} u_s \tag{A2}$$

where τ_{co} is the critical threshold shear stress for slip, b is the slip length once slip begins, and u_s is the slip velocity. (In the predictions shown in this paper, R_f was always taken to be equal to R; i.e., the whole contact was assumed filled with fluid. In practice, however, the predicted pressure and load are quite insensitive to the value of R_f so long as $R_f > R/50$.)

(a) No-Slip Condition. From the equilibrium of an element of fluid

$$\partial\tau_r/\partial z = \partial p/\partial r \tag{A3}$$

Assuming the fluid rheological model, $\tau = \eta(\partial u/\partial z)$

$$\frac{\partial p}{\partial r} = \frac{\partial}{\partial z}\left(\eta \frac{\partial u}{\partial z}\right) \tag{A4}$$

Note that this equation is derived rigorously and the parabolic approximation justified by Vinogradova.[23] This equation is integrated twice, assuming that the viscosity does not vary though the thickness of the film in the z direction, to give

$$\eta u = \frac{\partial p}{\partial r}\frac{z^2}{2} + C_1 z + C_2 \tag{A5}$$

Applying the no-slip boundary conditions, i.e., $u = 0$ at $z = 0$ and $u = 0$ at $z = h$ gives

$$u = \frac{1}{2\eta}\frac{\partial p}{\partial r}(z^2 - zh) \tag{A6}$$

The outward flow through an annular element of radius r can be determined by integrating this velocity through the thickness of the film and multiplying by $2\pi r$.

$$\dot{q}_r = -2\pi r \frac{h^3}{12\eta}\frac{\mathrm{d}p}{\mathrm{d}r} \tag{A7}$$

From volume conservation, this flow must equal the volume of the fluid displaced by squeeze from the circular region of radius r, i.e.

$$-2\pi r \frac{h^3}{12\eta}\frac{\mathrm{d}p}{\mathrm{d}r} = -\pi r^2 \frac{\mathrm{d}h}{\mathrm{d}t} \tag{A8}$$

Putting $w = -\mathrm{d}h/\mathrm{d}t$ (w is positive for downward motion), the pressure gradient at radius r is

$$\frac{\mathrm{d}p_r}{\mathrm{d}r} = -\frac{6\eta w r}{h^3} \tag{A9}$$

This equation can easily be integrated analytically with boundary condition $p_r = 0$ at $r = R_f$ to yield first the pressure p_r and then the load support, W.

$$p_r = 3\eta w R\left(\frac{1}{h^2} - \frac{1}{h_{R_f}^2}\right) \tag{A10}$$

$$W = 6\pi\eta w R^2\left(\frac{1}{h_o} - \frac{1}{h_{R_f}}\right) \tag{A11}$$

Assuming $h_{R_f} \gg h_o$, this gives the widely used form

$$W = 6\pi\eta w R^2/h_o \tag{A12}$$

Before considering analysis with slip, it should be noted that the shear stress at the two surfaces, τ_s, can be determined from the velocity gradient at the surfaces via the relation $\tau_s = \eta(\mathrm{d}u/\mathrm{d}z)_{z=0,h}$. For the no-slip case, these velocity gradients can be found by differentiating eq A6 and yield

$$\tau_s = \frac{h}{2}\frac{\mathrm{d}p}{\mathrm{d}r} \tag{A13}$$

By elimination of $\mathrm{d}p_r/\mathrm{d}r$ from eqs A9 and A13, this gives

$$\tau_s = -3\eta w r/h^2 \tag{A14}$$

(b) Slip Only Possible at One Surface. There are two alternative approaches to solving the case when slip occurs, one using a shear stress boundary condition and the second using a slip velocity boundary condition. In this analysis the second approach is used. An example of the first has been presented elsewhere by one of the authors.[27]

If slip takes place at one surface at slip velocity u_s, the integration constants C_1 and C_2 in eq A5 can be determined assuming a fluid film velocity $u = 0$ at the lower no-slip surface and $u = u_s$ at the upper, slip surface. This yields

$$u = \frac{1}{2\eta}\frac{\partial p}{\partial r}(z^2 - zh) + u_s\frac{z}{h} \tag{A15}$$

As in the no-slip case, this can be integrated through the thickness of the film to determine the flow rate through an annulus at radius r

$$\dot{q}_r = 2\pi r\left(-\frac{h^3}{12\eta}\frac{\mathrm{d}p}{\mathrm{d}r} + \frac{u_s h}{2}\right) \tag{A16}$$

Equating this with the fluid displaced due to squeeze as in eq A8 gives

$$\frac{\mathrm{d}p_r}{\mathrm{d}r} = -\frac{6\eta w r}{h^3} + \frac{6\eta}{h^2}u_s \tag{A17}$$

In eq A17, u_s is unknown. It can be found by determining the shear stress at the slipping surface using $\tau_s = \eta(\mathrm{d}u/\mathrm{d}z)_{z=h}$ and obtaining $(\mathrm{d}u/\mathrm{d}z)_{z=h}$ by differentiating eq A15. This gives

$$\tau_s = +\frac{h}{2}\frac{\mathrm{d}p}{\mathrm{d}r} + \frac{u_s\eta}{h} \tag{A18}$$

However when slip takes place, $\tau_s = -\tau_c$, where τ_c is defined by the slip model A2, i.e.

$$+\frac{h}{2}\frac{\mathrm{d}p}{\mathrm{d}r} + \frac{u_s\eta}{h} = -\left(\tau_{co} + \frac{\eta}{b}u_s\right) \tag{A19}$$

(The negative sign is used to allow for the fact that shear stress on the fluid at the wall is actually negative; i.e., it restrains radial outward flow, and this was not taken account of in the slip model eq A2 where τ_{co} and b are assumed to have positive values.)

Combining eqs A17 and A19 to eliminate u_s gives

$$\frac{\mathrm{d}p_r}{\mathrm{d}r} = -\frac{6\eta w r}{h^3}\frac{(h+b)}{(h+4b)} - \frac{6b}{h(h+4b)}\tau_{co} \tag{A20}$$

For the case of $\tau_{co} = 0$ so that slip occurs over the whole contact, this can be integrated to give Vinogradova's load support expression for slip at one surface.[23] For finite τ_{co} however, slip occurs only when the shear stress at the appropriate surface reaches this critical value. From eq A14, slip takes place when

$$3\eta w r/h^2 > \tau_{co} \tag{A21}$$

In practice the pressure gradient and thus the shear stress are low both in the very center of the contact and at large radial distances and have a maximum at $h = 4h_o/3$ for the no-slip case. This means that with a limiting shear stress for slip criterion, slip will occur within an annular region close to and around the contact center.

(27) Spikes, H. A. *Proc. Inst. Mech. Eng., Part J* **2003**, *217*, 1.

The solution for pressure thus involves the determination of whether slip will occur at each radial position and local integration of either the no-slip, eq A9, or the slip, eq A20, as appropriate. This is not possible analytically but is very straightforward numerically by integrating inward from the edge of the contact, where $p_{R_f} = 0$.

An alternative arrangement of eq A20 is

$$\frac{dp_r}{dr} = -\frac{6\eta wr}{h^3} + \frac{6b}{h(h+4b)}\left(-\tau_{co} + \frac{3\eta wr}{h^2}\right) \qquad \text{(A22)}$$

which shows how the critical shear stress always serves to reduce the negative pressure gradient and thus the load support. From eq A21, slip only occurs if the term in the innermost brackets is greater than zero. This leads to a succinct form of the pressure gradient for the contact, allowing for both no-slip and slip

$$\frac{dp_r}{dr} = -\min\left(\left(\frac{6\eta wr}{h^3}\right), \left(\frac{6\eta wr}{h^3} - \frac{6b}{h(h+4b)}\left(-\tau_{co} + \frac{3\eta wr}{h^2}\right)\right)\right) \qquad \text{(A23)}$$

(c) Slip Equally Possible at Both Surfaces. The approach is very similar to the case of slip at one wall. The integration constants in eq A5 are determined using the boundary conditions $u = u_s$ at $z = 0$ and $u = u_s$ at $z = h$ (the two surfaces are assumed identical so that u_s must be the same for both). This gives

$$u = \frac{1}{2\eta}\frac{\partial p}{\partial r}(z^2 - zh) + u_s \qquad \text{(A24)}$$

Integrating through the film to find $\dot{q}_r$ and equating this to the fluid displaced by squeeze gives

$$\frac{dp_r}{dr} = -\frac{6\eta wr}{h^3} + \frac{12\eta}{h^2}u_s \qquad \text{(A25)}$$

Following a similar determination of τ_s to that for the one surface slip case to eliminate u_s eventually yields

$$\frac{dp_r}{dr} = -\frac{6\eta wr}{h^3} + \frac{12b}{h(h+6b)}\left(-\tau_{co} + \frac{3\eta wr}{h^2}\right) \qquad \text{(A26)}$$

or, allowing for slip and no-slip over the contact

$$\frac{dp_r}{dr} = -\min\left(\left(\frac{6\eta wr}{h^3}\right), \left(\frac{6\eta wr}{h^3} - \frac{12b}{h(h+6b)}\left(-\tau_{co} + \frac{3\eta wr}{h^2}\right)\right)\right) \qquad \text{(A27)}$$

Again, for the case of $\tau_{co} = 0$, so that slip occurs over the whole contact, this can be integrated to give Vinogradova's load support expression for slip at two surfaces (eq 2). For $b \gg h$ the equation tends to eq 4 for critical shear stress for slip.

The procedure for obtaining a solution for pressure and consequent load support from eq A27 is the same as for the slip at one wall case described above.

(d) Slip Possible with Different Facility at Both Surfaces. In this case, when slip occurs at both surfaces the velocity profile is given by

$$u = \frac{1}{2\eta}\frac{\partial p}{\partial r}(z^2 - zh) + (u_{s2} - u_{s1})\frac{z}{h} + u_{s1} \qquad \text{(A28)}$$

where u_{s2} and u_{s1} are the slip velocities at the lower and upper surfaces.

As in the previous cases, this can be differentiated to obtain the shear stress at each surface, which is then equated with the shear stress for slip of the new model, to give, for the lower and upper surfaces, respectively

$$+\frac{h}{2}\frac{dp}{dr} - \frac{(u_{s2} - u_{s1})\eta}{h} = -\left(\tau_{co1} + \frac{\eta}{b_1}u_{s1}\right) \qquad \text{(A29a)}$$

$$+\frac{h}{2}\frac{dp}{dr} + \frac{(u_{s2} - u_{s1})\eta}{h} = -\left(\tau_{co2} + \frac{\eta}{b_2}u_{s2}\right) \qquad \text{(A29b)}$$

where τ_{co1}, b_1 and τ_{co2}, b_2 are the critical shear stress for slip and the slip length at either surface.

The velocity, eq A28, can also be integrated to obtain the flow rate, which can be equated with the flow due to squeeze displacement to give

$$\dot{q}_r = 2\pi r\left(-\frac{h^3}{12\eta}\frac{dp}{dr} + \frac{(u_{s2} + u_{s1})h}{2}\right) = \pi r^2 w \qquad \text{(A30)}$$

Equations A29 and A30 both relate slip velocity to pressure gradient and can be solved simultaneously to give the pressure gradient shown in the fourth expression in eq A31 below. This overall equation represents the pressure gradient at any radial location, taking into account the possibility of no slip and slip at either or both walls. The fourth expression is symmetrical with respect to the two surfaces, in that it yields the same solution regardless of which surface is designated 1 or 2. Also, as required, when $b_1 = b_2$ and $\tau_{co1} = \tau_{co2}$, it reduces to eq A26, i.e., to the slip equally possible at both surfaces case.

$$\frac{dp_r}{dr} = -\min\left(\left(\frac{6\eta wr}{h^3}\right), \left(\frac{6\eta wr}{h^3} - \frac{6b_1}{h(h+4b_1)}\left(-\tau_{co1} + \frac{3\eta wr}{h^2}\right)\right), \left(\frac{6\eta wr}{h^3} - \frac{6b_2}{h(h+4b_2)}\left(-\tau_{co2} + \frac{3\eta wr}{h^2}\right)\right), \left(\frac{\frac{6\eta wr}{h^3} - \frac{6\eta}{h^2}\left(\frac{(1+A)(-\tau_{co1}h/\eta + B)}{((1-A) + h/b_1)} + B\right)}{1 + \frac{3(1+A)}{((1-A) + h/b_1)}}\right)\right) \qquad \text{(A31)}$$

where

$$A = \frac{\left(\frac{2}{h} + \frac{1}{b_1}\right)}{\left(\frac{2}{h} + \frac{1}{b_2}\right)}$$

and

$$B = -\frac{(\tau_{co2} - \tau_{co1})}{\left(\frac{2}{h} + \frac{1}{b_2}\right)}$$

LA034123J